SURFACE INSTABILITIES ON A THIN POWER-LAW FLUID DURING SPIN COATING

C.-I. Chen

Department of Industrial Management
I-Shou University
Kaohsiung County, Taiwan 84041, R.O.C.

M.-C. Lin *

Department of Mechanical Engineering
National Kaohsiung University of Applied Sciences
Kaohsiung, Taiwan 80778, R.O.C.

C.-K. Chen

Department of Mechanical Engineering
National Cheng Kung University
Tainan, Taiwan 70101, R.O.C.

ABSTRACT

The phenomena of surface instabilities in a thin power-law fluid during spin coating are investigated. The set of Navier-Stokes equations with non-Newtonian behavior in the region of low Reynolds number serves as a mathematical description of the physical systems. Long-wave perturbation analysis is proposed to derive an evolution equation of the Ostwald de-Waele type fluid to govern the propagation of surface waves. Weakly nonlinear dynamics of film flow is studied by the multiple scales method. The amplitude of instability is determined by a Ginzburg-Landau equation. The study reveals that the degree of power-law index plays a vital role in stabilizing the film flow. The shear-thinning fluid is more unstable than the shear-thickening fluid in the stability analysis. Further, the nonlinear wave speed in the supercritical stability region decreases with increasing values of power-law index.

Keywords: Nonlinear stability, Power-law fluid, Spin coating.

1. INTRODUCTION

The stability in a thin film during spin coating has received much attention due to its wide application in the MEMS technology and thin film materials technology [1-4]. A great number of theoretical studies and numerical analysis [5] which is related to rotating disk have been carried out for various fluids and the excellent comprehensive review has been conducted by Rajagopal [6]. Study on the hydrodynamic stability of a thin flow flowing on a rotating circular disk started with the pioneering works by Emslie *et al*. [7]. They presented a simple expression for predicting how arbitrary initial shape would change with a thin Newtonian liquid during spin coating. It is showed that a flat interface is the preferred shape at low Re number. This model has been employed in the subsequent investigations for film flow on a rotating disk. Higgins [8] used the asymptotic methods for low and high Reynolds numbers on an unsteady Newtonian liquid. This work showed that a flat interface is inappropriate at high Reynolds number due to the nonlinear effects of circumferential waves and helical waves. However, surface instabilities of non-Newtonian fluid often behave different from the ones of Newtonian fluid for a film flow. Thin films of various polymers used as photo resists, dielectrics and protective coating are deposited during spin coating. The substances used in the spin coating under consideration consist of viscous suspensions which exhibit rather pronounced non-Newtonian characteristics. A non-Newtonian fluid is one whose flow curve (shear stress versus shear rate) is nonlinear or does not pass through the origin. Such non-Newtonian fluids may be grouped into three general classes: (1) general Newtonian fluids (time independent) (2) time-dependent fluids (3) viscoelastic fluids. Many mathematical models have been proposed to describe the flow characteristics of simple non-Newtonian fluids with regard to spin coating [9-11]. In the processing range of many polymeric liquids and dispersions, the Ostwald de-Waele power-law model is a good approximation to the data from viscosity versus shear rate [12]. The power index n of shearing-thinning fluid varies from zero to unity and its apparent viscosity decreases with increasing shear rate. On the contrary, the power index n of shearing-thickening fluid is greater than unity and its apparent viscosity increases with increasing shear rate. When the power index equals to 1, the fluid shows Newtonian behavior.

When the wavelength of the surface waves is assumed to be sufficiently large and the perturbation amplitude α is greatly less then unity ($\alpha << 1$), the long-wavelength modes that give the smallest wave number are most likely to induce flow instability. Long-wave

* Corresponding author (limit168@kuas.edu.tw)

DOI : 10.1017/jmech.2014.39
Copyright © 2014 The Society of Theoretical and Applied Mechanics, R.O.C.
https://doi.org/10.1017/jmech.2014.39 Published online by Cambridge University Press

perturbation analysis is proposed to derive a generalized kinematic model of the physical system with a small Reynolds number. Benny [13] studied the finite amplitude stability of a viscous liquid film on an inclined plane by using a perturbation expansion technique at Reynolds numbers ranging from 0 to 10. In a subsequent theoretical analysis, Lin [14] derived an evolution equation for describing this weakly nonlinear development of relatively long waves by using the same Benny equation. Chen *et al*. [15] studied the nonlinear stability characterization of thin condensate falling film on the outer surface of a rotating vertical cylinder at Reynolds numbers ranging from 0 to 15. Theoretical analysis of the thin flow and the effects of rheological properties of the substances should facilitate the understanding and control of the processes. Two mathematical models have been proposed to describe the weakly nonlinear stability of Newtonian fluid and viscoelastic fluid with regard to spin coating [16,17]. In this research, the authors consider rheological properties of both shear thinning pseudoplastic fluid and shear thickening dilatants fluid during spinning coating process. The influence of the rotational motion and the power-law index of a liquid on the equilibrium finite amplitude is studied and characterized mathematically.

2. MATHEMATICAL FORMULATION

Consider the axisymmetric flow of a thin Ostwald de-Waele power-law fluid flowing on a rotating circular disk which rotates with constant angular velocity Ω^* (see Fig. 1). A variable with a superscript "*" represents a dimensional quantity. Here the cylindrical polar coordinate axes r^*, θ^*, z^* are chosen as the radial direction, the circumferential direction and the axial direction perpendicular to the plate, respectively. All associated physical properties and the rate of film flow are assumed to be constant (*i.e.* time-invariant) because of the steady mass flow source at the center of rotation. Let u^* and w^* be the velocity components in the radial direction r^* and the axial direction z^* of the disk, respectively.

The governing equations of continuity and motion can be expressed as

$$\frac{1}{r^*}\frac{\partial(r^*u^*)}{\partial r^*}+\frac{\partial w^*}{\partial z^*}=0 \tag{1}$$

$$\rho\left(\frac{\partial u^*}{\partial t^*}+u^*\frac{\partial u^*}{\partial r^*}+w^*\frac{\partial u^*}{\partial z^*}-\frac{v^{*2}}{r^*}\right)=-\frac{\partial p^*}{\partial r^*}+\frac{1}{r^*}\frac{\partial(r^*\tau_{r^*r^*})}{\partial r^*}+\frac{\partial^*\tau_{z^*r^*}}{\partial z^*}-\frac{1}{r^*}\tau_{\theta^*\theta^*} \tag{2}$$

$$\rho\left(\frac{\partial w^*}{\partial t^*}+u^*\frac{\partial w^*}{\partial r^*}+w^*\frac{\partial w^*}{\partial z^*}\right)=-\frac{\partial p^*}{\partial z^*}-\rho g+\frac{1}{r^*}\frac{\partial(r^*\tau_{r^*z^*})}{\partial r^*}+\frac{\partial\tau_{z^*z^*}}{\partial z^*} \tag{3}$$

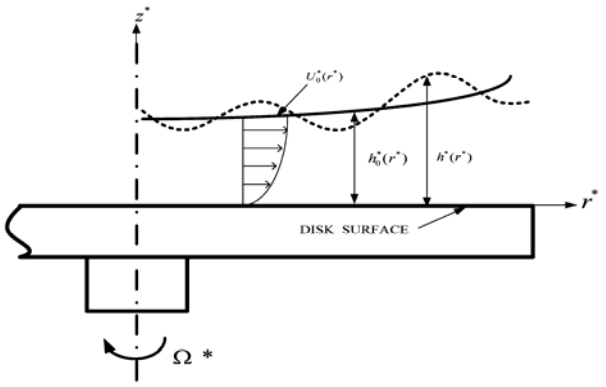


Fig. 1 Schematic diagram of a thin power-law fluid flowing on a rotating circular disk

where v^* is tangential velocity, ρ is constant fluid density, p^* is fluid pressure, g is acceleration due to gravity, μ_n is fluid dynamic viscosity and the individual stress components are given as

$$\tau_{r^*r^*}=2\mu_n\left(\frac{\partial u^*}{\partial r^*}\right)^n \tag{4}$$

$$\tau_{z^*z^*}=2\mu_n\left(\frac{\partial w^*}{\partial z^*}\right)^n \tag{5}$$

$$\tau_{r^*z^*}=\tau_{z^*r^*}=\mu_n\left(\frac{\partial u^*}{\partial z^*}+\frac{\partial w^*}{\partial r^*}\right)^n \tag{6}$$

$$\tau_{\theta^*\theta^*}=2\mu_n\left(\frac{u^*}{r^*}\right)^n \tag{7}$$

On the disk surface $z^*=0$, the boundary conditions are treated as no-slip as

$$u^*=0 \tag{8}$$

$$w^*=0 \tag{9}$$

On the free surface $z^*=h^*(r^*, t^*)$, the boundary condition approximated by the vanishing of the shear stress is expressed as

$$\left[1-\left(\frac{\partial h^*}{\partial r^*}\right)^2\right]\tau_{z^*r^*}+\frac{\partial h^*}{\partial r^*}(\tau_{z^*z^*}-\tau_{r^*r^*})=0 \tag{10}$$

The normal stress condition obtained by solving the balance equation in the direction normal to the free surface is given as

$$p^*+\left[1+\left(\frac{\partial h^*}{\partial r^*}\right)^2\right]^{-1}\left[2\tau_{z^*r^*}\frac{\partial h^*}{\partial r^*}-\tau_{z^*z^*}-\tau_{r^*r^*}\left(\frac{\partial h^*}{\partial r^*}\right)^2\right]+S^*\left\{\frac{\partial^2 h^*}{\partial r^{*2}}\left[1+\left(\frac{\partial h^*}{\partial r^*}\right)^2\right]^{-3/2}\right\}=p_a^* \tag{11}$$

https://doi.org/10.1017/jmech.2014.39 Published online by Cambridge University Press

The kinematic condition for a material free surface can be given as

$$\frac{\partial h^*}{\partial t^*}+\frac{\partial h^*}{\partial r^*}u^*-w^*=0 \tag{12}$$

where h^* is the local film thickness, S^* is surface tension and p_a^* is the atmospheric pressure. In order to reduce the subject quantifiable in the present study, the authors have used the mass-conservation equation to replace the two dependent velocity components u^*, w^* by the singe dependent stream function φ^* [13]. By introducing a stream function φ^*, the dimensional velocity components can be expressed as

$$u^*=\frac{1}{r^*}\frac{\partial \varphi^*}{\partial z^*},\ w^*=-\frac{1}{r^*}\frac{\partial \varphi^*}{\partial r^*} \tag{13}$$

The flow velocity (u^*, w^*) of Eq. (13) automatically satisfied the Eq. (1) of continuity when the existence of a stream function φ^*. The following variables are used to form the dimensionless governing equations and boundary conditions

$$z=\frac{z^*}{h_0^*},\ r=\frac{\alpha r^*}{h_0^*},\ t=\frac{\alpha t^* u_0^*}{h_0^*},\ h=\frac{h^*}{h_0^*},$$
$$\phi=\frac{\alpha\phi^*}{u_0^* h_0^{*2}},\ p=\frac{p^*-p_a^*}{\rho u_0^{*2}},\ \alpha=\frac{2\pi h_0^*}{\lambda} \tag{14}$$

where h_0^* is the average film thickness, α is the dimensionless wave number, λ is the wavelength, and u_0^* is the scale of velocity and defined as

$$u_0^*=\frac{n}{n+1}\left(\frac{g}{\nu_n}\right)^{1/n} h_0^{*(n+1)/n}$$

where ν_n is the kinematic viscosity,

The dimensionless parameter S (surface tension number) is defined as

$$S=\frac{S^*}{\rho u_0^{*2} h_0^*}$$

Re_n is the Reynolds number

$$\mathrm{Re}_n=\frac{u_0^{*2-n} h_0^{*n}}{\nu_n}$$

Fr is the Froude number

$$Fr=\frac{u_0^{*2}}{g h_0^*}=\left(\frac{n}{1+2n}\right)^n \mathrm{Re}_n$$

In order to investigate the effect of angular velocity, Ω^*, on the stability of the flow field, it is assumed that the azimuthal velocity is constant [11,15] throughout the radial direction in the thin film, *i.e.* $v^*=r^*\Omega^*$. The dimensionless parameter Ro (rotation number) is defined as

$$Ro=\frac{\Omega^* h_0^*}{u_0^*}$$

In terms of these non-dimensional variables, the equations of motion can be expressed as

$$r^{-1}\varphi_{zzz}=-\frac{\mathrm{Re}_n\cdot r\cdot Ro^2}{n}+\alpha\frac{\mathrm{Re}_n}{n}(p_r+r^{-1}\varphi_{tz}+r^{-2}\varphi_z\varphi_{rz}$$
$$-r^{-3}\varphi_z^2-r^{-2}\varphi_r\varphi_{zz})+O(\alpha^2) \tag{15}$$

$$p_z=-\mathrm{Re}_n^{-1}\left(\frac{1+2n}{n}\right)^n+\alpha\left(\mathrm{Re}_n^{-1}(n-2)r^{-1}\varphi_{rzz}\right)+O(\alpha^2) \tag{16}$$

Using the non-dimensional variables, the boundary conditions at the surface of the disk $z=0$ reduce to

$$\phi=\phi_r=\phi_z=0 \tag{17}$$

and the boundary conditions at the free surface of the disk $z=h$ become

$$r^{-1}\phi_{zz}=\alpha^2\left[r^{-1}\phi_{rr}-r^{-2}\phi_r+2h_r(1-\alpha^2h_r^2)^{-1}(2r^{-1}\phi_{rz}-r^{-2}\phi_z)\right] \tag{18}$$

$$p=-S\alpha^2h_{rr}(1+\alpha^2h_r^2)^{-3/2}$$
$$+\alpha\left[-2\mathrm{Re}_n^{-1}(1+\alpha^2h_r^2)^{-1}\left(r^{-1}\varphi_{rz}+r^{-1}(\varphi_{zz})^n h_r\right)\right]+O(\alpha^2) \tag{19}$$

$$h_t+r^{-1}h_r\phi_z+r^{-1}\phi_r=0 \tag{20}$$

In practice, the parameter S has a large value and $\alpha \ll 1$, so the term $\alpha^2 S$ is taken to be of order one [15-18]. In the present analysis, long-wave perturbation analysis is used to find out the asymptotic solutions of the above governing equation together with boundary conditions, this can be done by expanding the stream function and flow pressure in terms of a power series of α as

$$\phi=\phi_0+\alpha\phi_1+O(\alpha^2) \tag{21}$$

$$p=p_0+\alpha p_1+O(\alpha^2) \tag{22}$$

The flow conditions of the thin film can be obtained by inserting the above expressions into Eqs. (15) ~ (20) and then solving systematically the resulting equations. By collecting all terms of zeroth order α^0 and first order α^1 in the above governing equations and boundary conditions, the solutions of the zeroth order and first order equations were obtained and are given in Appendix A.

The zeroth order and first order solutions are inserted into the dimensionless free surface kinematic equation to yield the following generalized nonlinear kinematic equation

$$h_t+A(h)h_r+B(h)h_{rr}+C(h)h_{rrr}$$
$$+D(h)h_{rrrr}+E(h)h_r^2+F(h)h_rh_{rrr}=0 \tag{23}$$

https://doi.org/10.1017/jmech.2014.39 Published online by Cambridge University Press

where $A(h)$, $B(h)$, $C(h)$, $D(h)$, $E(h)$ and $F(h)$ are given in Appendix B. When the power-law index, n approaches unity, the fluid flow is reduced to the typical Newtonian film flow [16].

3. STABILITY ANALYSIS

The analysis in the present study is based on the locally valid unsteady equation under the assumption of steady state undisturbed liquid film. The dimensionless film thickness, when expressed in terms of the perturbed variables can be given as

$$h(r,t) = 1 + \eta(r,t) \tag{24}$$

where η is a perturbed quantity to the stationary film thickness. Substituting the value of $h(r, t)$ into the evolution Eq. (23) and all terms up to order η^3 are collected, the evolution equation of η becomes

$$\begin{aligned}&\eta_t + A\eta_r + B\eta_{rr} + C\eta_{rrr} + D\eta_{rrrr} + E\eta_r^2 + F\eta_r\eta_{rrr}\\ &= \left(A'\eta + \frac{A''}{2}\eta^2\right)\eta_r + \left(B'\eta + \frac{B''}{2}\eta^2\right)\eta_{rr}\\ &\quad + \left(C'\eta + \frac{C''}{2}\eta^2\right)\eta_{rrr} + \left(D'\eta + \frac{D''}{2}\eta^2\right)\eta_{rrrr}\\ &\quad + (E + E'\eta)\eta_r^2 + (F + F'\eta)\eta_r\eta_{rrr} + O(\eta^4)\end{aligned} \tag{25}$$

where the values of A, B, C, D, E, F and their derivatives are all evaluated and as following at the dimensionless height of the film $h = 1$.

3.1 Linear Stability Analysis

When the nonlinear terms of Eq. (25) are neglected, the linearized equation is given as

$$\eta_t + A\eta_r + B\eta_{rr} + C\eta_{rrr} + D\eta_{rrrr} = 0 \tag{26}$$

In order to use the normal mode analysis, we assume that

$$\eta = a\exp\left[i(r - dt)\right] + c.c. \tag{27}$$

where a is the perturbation amplitude, and c.c. is the complex conjugate counterpart. The complex wave celerity, d is given as

$$d = d_r + id_i = (A - C) + i(B - D) \tag{28}$$

where d_r and d_i are the linear wave speed and linear growth rate of the disturbance respectively. The solution of the disturbance about $h(r, t) = 1$ is asymptotically stable or unstable according as $d_i < 0$ or $d_i > 0$. This is equivalent to the inequality $B < D$ or $B > D$.

3.2 Weakly Nonlinear Stability Analysis

Nonlinear effects, when they are sufficiently weak, do not fundamentally alter the nature of the motion. A weakly nonlinear solution can be usefully expressed as weak stability or instability, but the definition is restricted to some neighborhood of critical value [19]. In this paper the authors are interested in investigating the existence of the supercritical and subcritical regions. In order to characterize the weakly nonlinear behavior of the thin film flows, the method of multiple scales [20] is employed here, as a result, of the Ginburg-Landau equation [21] can be derived following the same procedure as [17].

$$\frac{\partial a}{\partial t_2} + D_1\frac{\partial^2 a}{\partial r_1^2} - \varepsilon^{-2}d_i\, a + (E_1 + iF_1)a^2\bar{a} = 0 \tag{29}$$

where ε is a small perturbation parameter, $t_2 = \varepsilon^2 t$, $r_1 = \varepsilon r$, and

$$\begin{aligned}e = e_r + ie_i &= \frac{(B' - D' + E - F)(16D - 4B) + 6C(A' - C')}{(16D - 4B)^2 + 36C^2}\\ &\quad + i\frac{6C(B' - D' + E - F) - (A' - C')(16D - 4B)}{(16D - 4B)^2 + 36C^2}\end{aligned} \tag{30}$$

$$D_1 = \left[(B - 6D) + i(3C)\right] \tag{31}$$

$$\begin{aligned}E_1 &= (-5B' + 17D' + 4E - 10F)\, e_r - (A' - 7C')\, e_i\\ &\quad + \left(-\frac{3}{2}B'' + \frac{3}{2}D'' + E' - F'\right)\end{aligned} \tag{32}$$

$$\begin{aligned}F_1 &= (-5B' + 17D' + 4E - 10F)\, e_i\\ &\quad + (A' - 7C')\, e_r + \frac{1}{2}(A'' - C'')\end{aligned} \tag{33}$$

The overhead bar appearing in Eq. (29) stands for the complex conjugate of the same variable. Equation (29) can be used to investigate the weak nonlinear behavior of the fluid film flow. In order to solve for Eq. (29), we assume a filtered wave with no spatial modulation, so the filtered wave can be expressed as

$$a = a_0\exp\left[-ib(t_2)\, t_2\right] \tag{34}$$

After substituting Eq. (34) into Eq. (29), one can obtain

$$\frac{\partial a_0}{\partial t_2} = (\varepsilon^{-2}d_i - E_1 a_0^2)\, a_0 \tag{35}$$

$$\frac{\partial\left[b(t_2)\, t_2\right]}{\partial t_2} = F_1\, a_0^2 \tag{36}$$

The associated wave amplitude εa_0 in the supercritical stable region is derived and given as

$$\varepsilon a_0 = \sqrt{\frac{d_i}{E_1}} \tag{37}$$

If $E_1 = 0$, then Eq. (35) is reduced to a linear equation. The second term on the right-hand side of Eq. (35) is due to the nonlinearity and may moderate or

https://doi.org/10.1017/jmech.2014.39 Published online by Cambridge University Press

accelerate the exponential growth of the linear disturbance according to the signs of d_i and E_1. Equation (35) is used to modify the perturbed wave speed caused by infinitesimal disturbances appearing in the nonlinear system. The condition for the film flow to present the behavior of sub-critical instability in the linearly stable region ($d_i < 0$) is given as $E_1 < 0$, and the threshold amplitude of the wave is given as εa_0. The sub-critical stable region can only be found as $E_1 > 0$. The neutral stability curve can only be derived and plotted for the condition of $E_1 = 0$. The Ginzburg-Landau equation can be used to characterize various flow states with the results summarized in Table 1.

Table 1 Various states of Landau equation

linearly stable (subcritical region) $d_i < 0$	subcritical instability $E_1 < 0$	$\varepsilon a_0 < (d_i / E_1)^{1/2}$	$a_0 \to 0$	Conditional stability
		$\varepsilon a_0 > (d_i / E_1)^{1/2}$	$a_0 \uparrow$	Subcritical explosive state
	subcritical (absolute) stability $E_1 > 0$	$a_0 \to 0$		
Linearly unstable (supercritical region) $d_i > 0$	supercritical explosive state $E_1 < 0$	$a_0 \uparrow$		
	supercritical stability $E_1 > 0$	$\varepsilon a_0 \to (d_i / E_1)^{1/2}$		

4. NUMERICAL EXAMPLES

Each type of non-Newton fluid which is represented by various power law index n must be evaluated directly. In the present study, the selected reference fluid [22,23] has density $\rho = 0.98 \times 10^3 \text{kg/m}^3$, fluid dynamic viscosity $\mu_n = 0.79\text{N s/m}^2$ and a film of this mixture with thickness of the order $h_0^* = 10^{-2}\text{m}$. Due to the effects of rotation number and disk size on the stability of the film flows are well-known [16,17], the authors are interested in investigating the effect of power-law index on the stability of a thin flow. For the purposes of comparison, the physical parameters and their value range for the numerical experiments are based on the literatures [16,17]. More specifically, these parameters and their values include: (1) Reynolds number ranges from 0 to 15; (2) dimensionless perturbation wave numbers range from 0 to 0.12; (3) rotation numbers are 0.1 and 0.12, respectively. (4) power-law index n are 0.9, 0.95, 1.0, and 1.1, respectively. The remaining parameters are treated as constants for all numerical computations since we are considering practical spin coating systems in which these variables are not expected to undergo significant variation. Further, for a simplified analysis, $\alpha^2 S$ and Re_n are taken to be of the same order (***O*** (1)), the dimensionless surface tension $S = 6173.5$ and the dimensionless radius $r = 50$ [15,16].

4.1 Linear Stability Analysis

By setting $d_i = 0$ in the linear stability analysis, the neutral stability curve can be determined from Eq. (28). The $\alpha^2 S - \text{Re}_n$ plane is divided into two different characteristic regions by the neutral stability curve. One is the linearly stable region where small disturbances decay with time and the other is the linearly unstable region where small perturbations grow as time increases. Figure 2(a) shows that the stable region increases and unstable region decreases with an increase of power-law index. The microstructure characteristic of the power-law fluid suppresses the convective motion of the flow because the effective viscosity will increase when n increases. The results of the linear stability analysis are in agreement with those of Cheng and Liu [18] and Dandapat and Mukhopadhyay [24]. Figure 2(b) shows the temporal growth rate of a power-law

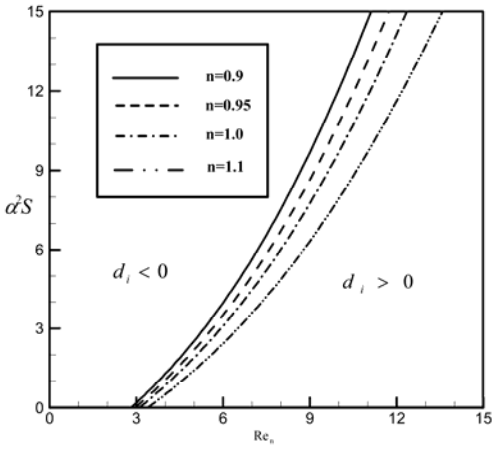


Fig. 2(a) Linear neutral stability curves for four different n values at $r = 50$ and $Ro = 0.1$

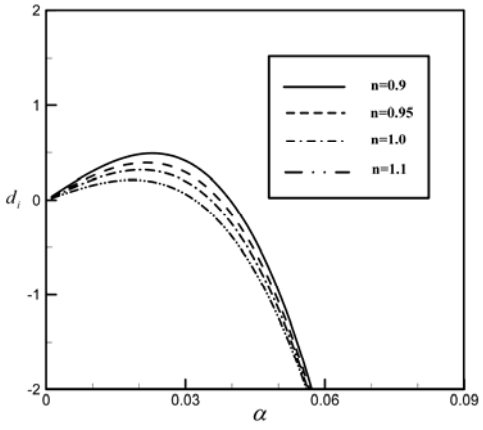


Fig. 2(b) Amplitude growth rate of disturbed wave for $Ro = 0.1$, $r = 50$ and $\text{Re}_n = 9$

fluid during spin coating at n = 0.9, 0.95, 1.0 and 1.1, respectively. It is found that temporal growth rate decreases as the value of n increase. The shear-thinning fluid is more unstable than the shear-thickening fluid. Hence one can say that in linear stability analysis the degree of power-law index plays a vital role in stabilizing the film flow either in pseudo-plastic fluid or in dilatant fluid.

https://doi.org/10.1017/jmech.2014.39 Published online by Cambridge University Press

4.2 Weakly Nonlinear Stability Analysis

Figure 3(a) shows the threshold amplitude in sub-critical instability region for various wave numbers with different n values at $Ro = 0.1$, $r = 50$ and $\mathrm{Re}_n = 3$. The results indicate that the threshold amplitude εa_0 becomes smaller as the value of power-law index decreases. The film flow which holds the higher threshold amplitude value will become more stable than those that hold smaller one. If the initial finite-amplitude disturbance is less than the threshold amplitude, the system will become conditionally stable.

Figure 3(b) shows the threshold amplitude in the supercritical stability region for various wave numbers with different n values at $Ro = 0.12$, $r = 50$ and $\mathrm{Re}_n = 9$. It is found that increasing the power-law index will lower the threshold amplitude, whereupon the flow becomes relatively more stable. Figure 3(c) shows the nonlinear wave speed in the supercritical stable region for various wave numbers with different n values at $Ro = 0.12$, $r = 50$ and $\mathrm{Re}_n = 9$. It is found that the nonlinear wave speed increases as the power-law index decreases.

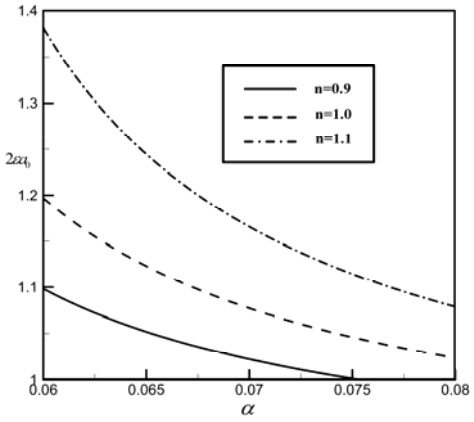


Fig. 3(a) Threshold amplitude in sub-critical instability region for three different n values at $Ro = 0.1$, $r = 50$ and $\mathrm{Re}_n = 3$

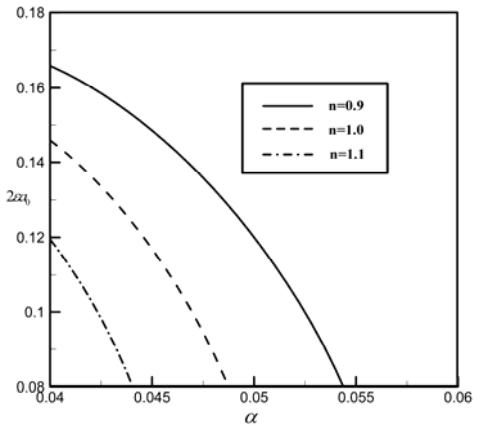


Fig. 3(b) Threshold amplitude in supercritical stability region for three different n values at $Ro = 0.12$, $r = 50$ and $\mathrm{Re}_n = 9$

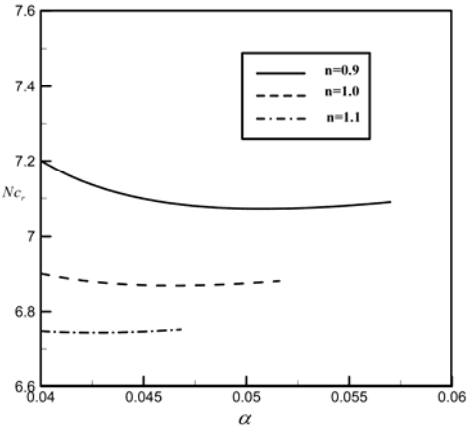


Fig. 3(c) Nonlinear wave speed in supercritical stability region for three different n values at $Ro = 0.12$, $r = 50$ and $\mathrm{Re}_n = 9$

5. CONCLUDING REMARKS

In order to simplify the analysis and computations, a number of assumptions have been made in the present study. In particular, the dimensions of the flow consistency coefficient depend on the numerical value of the power-law index n and therefore the flow consistency coefficient must not be compared when the n values differ. Generally, the Ostwald de-Waele type fluid applies over only a limited range of shear rates. Furthermore, it does not predict the zero and infinite shear viscosities. Also, the disk radius is much larger than the film thickness so that the peripheral effects are confined to a small region of the total film area and can be negligible. On the basis of the above assumptions, the finite amplitude and monochromatic wave is obtained. The surface instabilities of a thin power-law fluid during spin coating are investigated using the method of long-wave perturbation. On the basis of the results of numerical modeling, several conclusions can be drawn:

1. For both pseudoplastic fluid and dilatant fluid, the power law index n plays a vital role in stabilizing the film flow. The greater the n value is, the more stable the film flow is.
2. The shear-thinning fluid is more unstable than the shear-thickening fluid in the stability analysis.
3. From weakly nonlinear analysis, the effective viscosity increases with increasing power law index n. And this will decrease the nonlinear wave speed of fluid system to reach the supercritical stability easily.

ACKNOWLEDGEMENTS

The authors sincerely thank the anonymous reviewers for their valuable comments and suggestions which have helped in improving the quality of this manuscript. Also, this work was supported by the National Science Council of the Republic of China under grant NSC Project No. 101-2221-E-214-020.

https://doi.org/10.1017/jmech.2014.39 Published online by Cambridge University Press

APPENDIX A

Zeroth-order Solution:

$$\varphi_0 = \frac{r^2 \cdot \mathrm{Re}_n \cdot Ro^2 (3h - z)\, z^2}{6n}$$

where the zero-order governing equation

$$r^{-1}\varphi_{0zzz} = -\frac{\mathrm{Re}_n \cdot r \cdot Ro^2}{n}$$

$$p_{0z} = -\mathrm{Re}_n^{-1}\left(\frac{1+2n}{n}\right)^n$$

Associated with boundary condition

$$z = 0 \qquad \phi_0 = \phi_{0z} = 0$$

$$z = h \qquad r^{-1}\phi_{0zz} = 0$$

$$p_0 = -\alpha^2 S\, h_{rr}$$

First-order solution:

$$\varphi_1 = k_1 z^8 + k_2 z^7 + k_3 z^6 + k_4 z^5 + k_5 z^4 + k_6 z^3 + k_7 z^2 + k_8 z + k_9$$

where

$$k_1 = -\frac{r^2 \cdot \mathrm{Re}_n^3 \cdot Ro^4}{2016 n^3} \qquad k_2 = \frac{(1+5h)\, r^2 \cdot \mathrm{Re}_n^3 \cdot Ro^4}{1260 n^3} \qquad k_3 = \frac{-h(2+3h)\, r^2 \cdot \mathrm{Re}_n^3 \cdot Ro^4}{360 n^3}$$

$$k_4 = \frac{h \cdot r^2 \cdot \mathrm{Re}_n^3 \cdot Ro^4 (2h + r h_r)}{120 n^3} \qquad k_5 = -\frac{h^2 \cdot r^2 \cdot \mathrm{Re}_n^3 \cdot Ro^4 (2h + 3r h_r)}{72 n^3} \qquad k_6 = \frac{r\left(\left(2+\frac{1}{n}\right)^n h_r - \mathrm{Re}_n \cdot S \cdot \alpha^2 \cdot h_{rrr}\right)}{6n}$$

$$k_7 = \frac{1}{90 n^3}\left(h \cdot r\left(h^4 (6+5h) r \cdot \mathrm{Re}_n^3 \cdot Ro^4 + \left(-45\left(2+\frac{1}{n}\right)^n n^2 + 15 h^3 \cdot r^2 \cdot \mathrm{Re}_n^3 \cdot Ro^4\right) h_r + 45 n^2\, \mathrm{Re}_n \cdot S \cdot \alpha^2 h_{rrr}\right)\right)$$

$$k_8 = k_9 = 0$$

where the first-order governing equation

$$r^{-1}\varphi_{1zzz} = \frac{\mathrm{Re}_n}{n}(p_{0r} + r^{-1}\varphi_{0tz} + r^{-2}\varphi_{0z}\varphi_{0rz} - r^{-3}\varphi_{0z}^2 - r^{-2}\varphi_{0r}\varphi_{0zz})$$

$$p_{1z} = \mathrm{Re}_n^{-1}(n-2)\, r^{-1}\phi_{0rzz}$$

Associated with boundary condition

$$z = 0 \qquad \phi_0 = \phi_{0z} = 0$$

$$z = h \qquad r^{-1}\phi_{1zz} = 0$$

$$p_1 = -2\,\mathrm{Re}_n^{-1}\left(r^{-1}\phi_{0rz} + r^{-1}(\phi_{0zz})^n h_r\right)$$

https://doi.org/10.1017/jmech.2014.39 Published online by Cambridge University Press

APPENDIX B

$$A(h)=\frac{h^2\left(h^4(136+73h)\,r^2\cdot Re_n{}^3\cdot Ro^4\cdot\alpha+60n^2\left(3r^2\cdot \mathrm{Re}_n\cdot Ro^2-h\left(2+\frac{1}{n}\right)^n\cdot\alpha\right)\right)}{180n^3\cdot r}$$

$$B(h)=\frac{h^3\left(-5\left(2+\frac{1}{n}\right)^n n^2+2h^3\cdot r^2\cdot \mathrm{Re}_n{}^3\cdot Ro^4\right)\alpha}{15n^3}$$

$$C(h)=\frac{S\cdot \mathrm{Re}_n\cdot h^3\alpha^3}{3\mathrm{n}\cdot \mathrm{r}}$$

$$D(h)=\frac{S\cdot \mathrm{Re}_n\cdot h^3\alpha^3}{3\mathrm{n}}$$

$$E(h)=\frac{h^2\left(-5\left(2+\frac{1}{n}\right)^n n^2+4h^3\cdot r^2\cdot \mathrm{Re}_n{}^3\cdot Ro^4\right)\alpha}{5n^3}$$

$$F(h)=\frac{\mathrm{Re}_n\cdot S\cdot h^2\alpha^3}{n}$$

REFERENCES

1. Kitamura, A., Hasegawa, E. and Yoshizawa, M., "Asymptotic Analysis of the Formation of Thin Liquid Film in Spin Coating," *Fluid Dynamic Research*, **30**, pp. 107–125 (2002).
2. Sisoev, G. M., Matar, O. K. and Lawrence, C. J., "Stabilizing Effect of the Coriolis Forces on a Viscous Liquid Film Flowing over a Spinning Disc," *Comptes Rendus Mechanique*, **332**, pp. 203–207 (2004).
3. Kuo, Y. K. and Chao, C. G., "Control Ability of Spin Coating Planarization of Resist Film and Optimal of Developers," *Microelectronics Journal*, **37**, pp. 759–764 (2006).
4. Li, Y., Ma, M., Wang, X. and Li, Z., "Preparation of Cerium-Doped Titania Macroporus Films by a Sol-Gel Spin Coating Using Polypropylene Glycol (PPG) as Pore-Creating Agent: Effects of Ce Ions, PPG and Calculation on Photocatalytic Activity," *Surface & Coating Technology*, **204**, pp. 1353–1358 (2010).
5. Lai, C. Y., Rajagopal, K. R. and Szeri, A. Z., "Asymmetric Flow Above a Rotating Disk," *Journal of Fluid Mechanics*, **157**, pp. 471–492 (1985).
6. Rajagopal, K. R., "Flow of Viscoelastic Fluids Between Rotating Disks," *Theoretical and Computational Fluid Dynamics*, **3**, pp. 185–206 (1992).
7. Emslie, A. G., Bonner, F. T. and Peck, L. G., "Flow of a Viscous Liquid on a Rotating Disk," *Journal of Applied Physics*, **29**, pp. 858–862 (1958).
8. Higgins, B. G., "Film Flow on a Rotating Disk," *Physics Fluids*, **29**, pp. 3522–3529 (1986).
9. Acrivos, A., Shah, M. J. and Petersen, E. E., "On the Flow of a Non-Newtonian Liquid on a Rotating Disk," *Journal of Applied Physics*, **31**, pp. 963–968 (1960).
10. Burgess, S. L. and Wilson, S. D. R., "Spin-Coating of a Viscoplastic Material," *Physics Fluids*, **8**, pp. 2291–2297 (1996).
11. Hayat, T., Javed, T. and Sajid, M., "Analytic Solution for MHD Rotating Flow of a Second Grade Fluid over a Shrinking Surface," *Physics Letters A*, **372**, pp. 3264–3273 (2008).
12. Chhabra, R. P. and Richardson, J. F., *Non-Newtonian Flow and Applied Rheology: Engineering Applications*, 2nd Edition, Butterworth-Heinemann, U.K. (2008).
13. Benney, D. J., "Long Waves on Liquid Films," *Journal of Mathematics Physics*, **45**, pp. 150–155 (1966).
14. Lin, S. P., "Finite Amplitude Sine-Band Stability of a Viscous Film," *Journal of Fluid Mechanics*, **63**, pp. 417–429 (1974).
15. Chen, C. I., Chen, C. K. and Yang, Y. T., "Perturbation Analysis to the Nonlinear Stability Characterization of Thin Condensate Falling Film on the Outer Surface of a Rotating Vertical Cylinder," *International Journal of Heat and Mass Transfer*, **47**, pp. 1937–1951 (2004).
16. Chen, C. K. and Lin, M. C., "Weakly Nonlinear Hydrodynamic Stability of Thin Newtonian Fluid Flowing on a Rotating Circular Disk," *Mathematical Problems in Engineering*, DOI:10.1155/2009/948672 (2009).
17. Lin, M. C. and Chen, C. K., "Finite Amplitude Long-Wave Instability of a Thin Viscoelastic Fluid During Spin Coating," *Applied Mathematical Modelling*, **36**, pp. 2536–2549 (2012).
18. Cheng, P. J. and Liu, K. C., "Hydromagnetic Instability of a Power-Law Liquid Film Flowing Down a Vertical Cylinder Using Numerical Approximation Approach Techniques," *Applied Mathematical Modeling*, **33**, pp.1904–1914 (2009).
19. Eckhaus, W., *Studies in Nonlinear Stability Theory*,

https://doi.org/10.1017/jmech.2014.39 Published online by Cambridge University Press

Springer, Berlin (1965).
20. Krishna, M. V. G. and Lin, S. P., "Nonlinear Stability of a Viscous Film with Respect to Three-Dimensional Side-Band Disturbance," *Physics of Fluids*, 20, pp. 1039–1044 (1977).
21. Ginzburg, V. L. and Landau, L. D., "Theory of Superconductivity," *Journal of Experiential Theoretic Physics (USSR)*, **20**, pp. 1064–1082 (1950).
22. Anderson, H. I. and Dahi, E. N., "Gravity-Driven Flow of a Viscoelastic Liquid Film Along a Vertical Wall," *Journal Physical D: Applied Physics*, **32**, pp. 1557–1562 (1999).
23. Uma, B. and Usha, R., "Interfacial Phase Change Effects on the Stability Characteristics of Thin Viscoelastic Liquid Film Down a Vertical," *International Journal of Engineering Science*, **42**, pp. 1381–1406 (2004).
24. Dandapat, B. S. and Mukhopadhyay, A., "Waves on the Surface of a Falling Power-Law Fluid Film," *International Journal of Non-linear Mechanics*, **38**, pp. 21–38 (2003).

(Manuscript received May 18, 2013,
accepted for publication February 11, 2014.)

https://doi.org/10.1017/jmech.2014.39 Published online by Cambridge University Press